Ion Channel Block by Acetylcholine, Carbachol and Suberyldicholine at the Frog Neuromuscular Junction

D. C. Ogden, D. Colquhoun

Proceedings of the Royal Society of London. Series B, Biological Sciences, Volume 225, Issue 1240 (Sep. 23, 1985), 329-355.

Proc. R. Soc. Lond. B **225**, 329–355 (1985)
Printed in Great Britain

Ion channel block by acetylcholine, carbachol and suberyldicholine at the frog neuromuscular junction

BY D. C. OGDEN AND D. COLQUHOUN†

M.R.C. Receptor Mechanisms Research Group, Department of Pharmacology, University College London, Gower Street, London WC1E 6BT, U.K.

(*Communicated by H. P. Rang, F.R.S. – Received* 1 *February* 1985)

Three nicotinic agonists, suberyldicholine, acetylcholine and carbachol, have been investigated by single channel recording at the endplates of adult frog muscle fibres. All three agonists can block the channels that they open. Suberyldicholine is the most potent blocker; it has an equilibrium constant for binding to the open channel of about 6 μM and blockages last for about 5 ms on average, at −105 mV. A plot of the mean number of blockages per unit open time against concentration ('blockage frequency plot') suggests that suberyldicholine does not produce long-lived blocked states such as might occur, for example, if it could be trapped within a shut channel. The characteristics of the 'blockage frequency plot' are analysed in Appendix 2. Block by acetylcholine and carbachol has much lower affinity (the equilibrium constants being a few millimolar for both), and blockages are much briefer, so that blockage appears to produce noisy single channel currents of reduced amplitude. A method based on the spectral density of the excess 'open' channel noise has been used to investigate the rate of blocking and unblocking. The basis of this method is discussed in Appendix 1. It is estimated that the mean duration of a blockage is about 18 μs for acetylcholine and 9 μs for carbachol.

INTRODUCTION

A wide range of small organic molecules has been found to block open agonist-activated ion channels. At the skeletal neuromuscular junction, this effect is produced, for example, by local anaesthetics (Adams 1977; Neher & Steinbach 1978; Ogden *et al.* 1981) and as an additional action of classical competitive antagonists (Katz & Miledi 1978; Colquhoun *et al.* 1979; Colquhoun & Sheridan 1981). There has, however, been relatively little work on block by agonists that open the channels.

It has been reported that suberyldicholine (SubCh) in high concentrations produces an inverse relaxation of current characteristic of channel block following a voltage step at the frog endplate (Adams 1976) and that acetylcholine (ACh) and carbachol (CCh) may act in a similar way but faster, (Adams & Colquhoun 1983; Colquhoun & Ogden 1984). The kinetics of block of frog endplate channels by decamethonium have been estimated from noise and relaxation experiments by Adams & Sakmann (1978), and recent work by Sine & Steinbach (1984) has

† Elected F.R.S. 21 March 1985.

described channel block by SubCh, ACh and CCh of nicotinic ion channels in the BC3H1 cell line.

It is our aim in this paper to describe the equilibrium and kinetic properties of channel block by SubCh, ACh and CCh at the endplate of adult frog muscle fibres, and to consider the evidence for the specificity of this block for the open state of the ion channel. To this end we introduce two methods: the 'blockage frequency plot', and the inference of the rate of block from the excess 'open' channel noise. The characteristics of these methods are analysed in the appendixes.

Methods

Experiments were done with twitch fibres of M. cutaneus pectoris or M. semitendinosus of *Rana temporaria*. Fibres were separated and the presynaptic nerve terminals removed by enzymatic digestion with collagenase (Sigma Type 1A) 0.2% and protease (Sigma type VII) 0.02% (Betz & Sakmann 1973). Ringer solution had the following composition NaCl 116.5 mM, KCl 2.5 mM, $CaCl_2$ 1.5 mM, HEPES 10 mM, tetrodotoxin 50 nM, pH 7.2. During recording fibres were depolarized by bathing in a high KCl Ringer containing 15 or 25 mM KCl (substituted for NaCl), to minimize the problems that arose from movement of the fibre when a patch pipette containing a high agonist concentration was brought close to the endplate. Drugs used were acetylcholine chloride (Sigma), carbamylcholine chloride (Koch Light), tetrodotoxin (Sankyo); suberyldicholine was a gift of Dr J. Heeseman and Dr B. Sakmann.

Patch pipettes were made from borosilicate glass and filled with a solution of the agonist in normal Ringer. Pipettes of high resistance (20–40 MΩ) were used to minimize diffusion of agonist from the end of pipette. High resolution patch clamp recordings from the postsynaptic membranes were made with methods described by Hamill *et al.* (1981). Data were recorded on f.m. tape. Membrane potential was measured with a microelectrode.

For single channel analysis the record was filtered at 3 kHz (−3 dB, 8 pole Bessel) and a continuous section of it digitized at 32 or 40 kHz. Amplitude and durations of openings and gaps were measured directly, by use of the system response to a step input to fit transitions, and so an idealized record of open and gap times was obtained. A minimum resolvable interval was imposed on the data, usually 50 μs for shut and 100 μs for open times, to give a consistent time resolution. Data were displayed as histograms of apparent open and gap times and probability density functions fitted to the data with the method of maximum likelihood.

The 'open times' in the idealized record will be longer than the true open times because they will often contain unresolved gaps; they are therefore referred to as *apparent open times*. The mean apparent open time was corrected for the presence of unresolved short gaps by extrapolation to zero time of the probability density function fitted to the apparent shut times to obtain estimates of the total number of gaps and the total shut time in the record. The total open time was calculated as the total length of the record minus the total shut time and the corrected mean open time was calculated by division of the total open time so found by the number

of openings (number of gaps + 1) in the record. These procedures are described in detail by Colquhoun & Sigworth (1983).

The variance and power spectrum of current noise in single channel records were obtained by filtering at 4 kHz or 8 kHz (−3 dB, 8 pole Butterworth filter), and then digitizing the data at 8192 Hz or 16384 Hz respectively. 512 point spectra were calculated and Lorentzian curves fitted to the data as described by Colquhoun *et al.* (1979).

The mean current during a burst of openings was obtained by integration of the record over a specified interval, either directly with an analogue integrator (time constant 10s) or by numerical integration of the digitized record.

Results

Experiments with suberyldicholine

The evidence for block of open ion channels was rather more direct for SubCh than for ACh or CCh.

Kinetic measurements

Single channel currents recorded at an endplate with a low concentration (50 nM) of SubCh are shown in figure 1*a*; they may be compared with those seen at a 2000-fold higher concentration (100 μM SubCh) shown in figure 1*b*. Currents recorded at the high concentration were much shorter in duration than those recorded at low concentrations. In figure 1 the mean apparent open time (see Methods) was 6.6 ms at the low concentration, but only 0.23 ms in 100 μM SubCh.

FIGURE 1. Single channel currents recorded in SubCh 50 nM (upper trace) and 100 μM (lower trace). Membrane potential −105 mV. Temperature 10 °C. Recording bandwidth d.c. −3 kHz (−3 dB, eight-pole Bessel).

Indeed many of the openings in 100 μM SubCh were so brief that they failed to reach their full amplitude because of the limited frequency response of the recording system. The distributions of apparent open times are shown in figure 2 for 50 nM and 100 μM SubCh and similar results for other SubCh concentrations are summarized in column 2 of table 1. Clearly the mean apparent open time decreases as concentration is increased. It was also found (see table 1) that two exponential components were needed to fit the distributions of apparent open time at concentrations less than 5 μM, but at higher concentrations of SubCh, no fast component was detectable in the distribution and a single exponential distribution

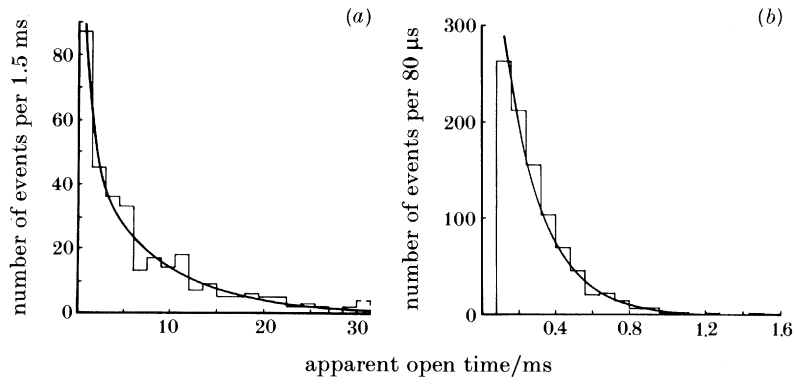

FIGURE 2. Histograms of apparent open times in SubCh (*a*) 50 nM (*b*) 100 μM. Potential −105 mV. Temperature 10 °C. Fitted curves: (*a*) sum of two exponentials with time constants 1.1 ms and 8.4 ms, and areas 0.22 and 0.78, respectively; (*b*) single exponential with time constant 0.21 ms.

TABLE 1. DISTRIBUTION OF SHUT AND OPEN TIMES WITH SUBERYLDICHOLINE

SubCh concentration	mean apparent open time	distribution of all shut times						corrected open time
		τ_1	area	τ_2	area	τ_3	area	
μM	ms	μs	(%)	ms	(%)	ms	(%)	ms
1	3.6	41	78	3.9	8	55	14	1.6
5	2.5	28	70	0.66	7	5.7	22	1.1
10	2.0	25	53	4.0	47	—	—	1.0
50	0.57	28	28	3.9	72	—	—	0.41
100	0.24	38	14	5.9	86	—	—	0.22

Membrane potential −105 mV. Temperature 10 °C. The time constants and areas of the components fitted to the distribution of all shut times within a cluster are shown. There is a component (shown underlined) with a time constant close to 5 ms in each case, and this component accounts for a progressively larger area as the concentration is increased. The distributions were used to correct the mean apparent open times (shown in column 2) for the effect of unresolved short gaps (see text). The corrected mean open times so found are shown in the last column.

provided a good fit (this is consistent with observations made by Colquhoun & Sakmann (1981, 1985)).

At concentrations of SubCh greater than 1 μM openings occurred in well-defined *clusters* of up to one second duration, which were separated by long gaps, as described for ACh by Sakmann *et al.* (1980). Within each cluster the distribution of gap durations showed two major exponential components, one with a time constant of 30–50 μs and the other with a time constant of 4–6 ms; the latter was undetectable at very low concentrations, but became more prominent as the SubCh concentration was increased. The time constants and relative areas of components of the gap distributions for SubCh at 1–100 μM, at a membrane potential of −105 mV, are summarized in table 1. The fraction of the area represented by the 4–6 ms components increased from 7.5% at 1 μM SubCh to 86% at 100 μM.

Furthermore the time constant for this component became longer as the membrane was hyperpolarized (it changed from 4–6 ms at −105 mV to 20.5 ms at −160 mV).

Thus, three features of these results suggest that SubCh blocks the open nicotinic ion channel: (i) the decrease in apparent open lifetime at high concentrations; (ii) the increase at high concentrations in the proportion of gaps that are assumed to correspond to channel blockages; and (iii) the increase in duration of these gaps as the membrane is hyperpolarized. These results are similar to those obtained with other putative open channel blockers (see, for example, Adams 1977; Neher & Steinbach 1978; Neher 1983; Ogden *et al.* 1981).

Two quantitative tests of the open channel block hypothesis were made. Before doing these tests, estimates were made of the number of gaps in the record that were too short to be detected. These undetected gaps will cause the mean apparent channel open time to be longer than the actual mean open lifetime, so a corrected mean open lifetime was then calculated, as described in the Methods section. Corrected mean open lifetimes at various SubCh concentrations are listed in column 6 of table 1. If we suppose that there is only one open state with a shutting rate constant α in the absence of block (mean lifetime, $1/\alpha$), then if a blocking molecule can combine with the open channel (with association rate constant k^*_{+B}), the mean open lifetime will be reduced to $1/(\alpha + k^*_{+B}\, x_B)$ where x_B is the concentration of the blocking molecule. (In fact the distribution of open lifetimes was not a single exponential at low agonist concentrations but the minor fast component is neglected in these calculations.) A plot of the reciprocal of the corrected mean open time against SubCh concentration (at −105 mV) is shown in figure 3 (closed circles). As predicted the points lie close to a straight line. The slope is $k^*_{+B} = (3.9 \pm 0.1) \times 10^7$ M^{-1} s^{-1}, and the intercept is $\alpha = (594 \pm 51)$ s^{-1} which is similar to the channel closing rate estimated at low (100 nM or less) SubCh concentrations (Colquhoun & Sakmann 1981).

Another useful test of the channel block hypothesis would be to measure the number of blockages per burst (a burst being defined here as the series of openings that result from a single activation of the channel), and the total open time per burst (see, for example, Neher 1983; Colquhoun & Hawkes 1983; Ogden *et al.* 1985). This, however, is not possible in the present case because block becomes prominent only at agonist concentrations that are so high that it is no longer possible to distinguish clearly when one burst ends and the next begins (see figure 1*b*). A different procedure was therefore adopted; in figure 3 (open circles) the number of blockages per unit open time is plotted against SubCh concentration. This was calculated by estimating the number of 4–6 ms gaps (putative blockages) from the fitted distribution of all shut times, and dividing by the total open time in the record (which was corrected for undetected gaps). This procedure does not require that separate activations be distinguishable from one another in the record. For a simple open channel blocking agent the block frequency per unit open time should be simply $k^*_{+B}\, x_B$. The slope of the line fitted in figure 3 is $(3.8 \pm 0.1) \times 10^7$ M^{-1} s^{-1} which does indeed agree well with the estimate of k^*_{+B} found above from open times; if the blocker could become trapped within a shut channel, or if the channel were able to shut directly from the blocked state without returning through the open

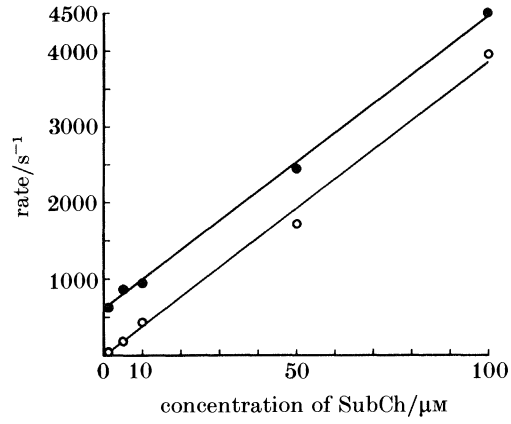

FIGURE 3. Effect of SubCh concentration on mean open time and on blockage frequency. Closed circles: reciprocal of corrected mean open time plotted against concentration. Line fitted to points by method of least squares; slope = $(3.9 \pm 0.1) \times 10^7$ M^{-1} s^{-1}, intercept = 594 ± 51 s^{-1}. Open circles: frequency of 4–6 ms gaps per unit open time during a cluster of openings plotted against concentration ('blockage frequency plot'). Line fitted by least squares; slope = $(3.8 \pm 0.1) \times 10^7$ M^{-1} s^{-1}, intercept = 4.1 ± 66 s^{-1}. Temperature 10 °C. Potential −105 mV.

state, a slope of less than k^*_{+B} would have been predicted under certain circumstances (see Discussion and Appendix 2).

The unblocking rate constant, k^*_{-B}, can be estimated (see Discussion) as the reciprocal of the mean lifetime of the 4–6 ms gaps which, according to the above analysis, appear to be channel blockages. This was $k^*_{-B} = 221 \pm 20$ s^{-1} at −105 mV. Combination of this value with a blocking rate constant of 3.9×10^7 M^{-1} s^{-1} gives an estimate of the equilibrium dissociation constant as $K^*_B = 5.7$ μM for SubCh at a membrane potential of −105 mV.

Equilibrium measurements

The proportion of the time for which the channel was open within clusters, p_o, at SubCh concentrations greater than 5 μM was calculated from the measured distribution of open and shut times. These values are given in table 2; p_o declined from 0.47 at 5 μM to 0.03 at 100 μM SubCh. There is some reason to believe that in this concentration range p_o would be close to 1.0 if it were not for block (see, for example, Colquhoun & Sakmann 1981, 1985). If this were true, and the reduction of p_o below 1.0 was a result of channel block, then we would expect that $(1-p_o)/p_o = x_B/K^*_B$. A Hill plot, of lg $[p_o/(1-p_o)]$ against log concentration, is shown in figure 4. It has a negative slope because we are looking at block rather than at activation. The slope of -1.06 ± 0.2 is consistent with the expected relationship. Furthermore, the value of $K^*_B = 5.8 \pm 1.6$ μM inferred from essentially equilibrium measurements in figure 4 is close to the value of 5.7 μM that was inferred above entirely from kinetic measurements.

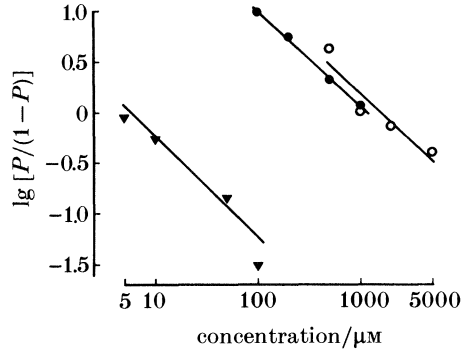

FIGURE 4. Hill plots of $\lg[p_o/(1-p_o)]$ against log concentration for SubCh (▼) ACh (●) and CCh (○). Potential −105 mV (SubCh), −100 mV to −120 mV (ACh) and −120 mV to −140 mV (CCh). Temperature 10–12 °C. Lines fitted by least squares. For SubCh, slope is -1.06 ± 0.2, intercept is 5.8 μM; for ACh, slope is -0.94 ± 0.04, intercept is 1.2 mM; for CCh slope is -0.96 ± 0.21, intercept is 1.6 mM.

TABLE 2. CHANNEL BLOCK AT EQUILIBRIUM BY ACh AND CCh

agonist	concentration mM	membrane potential mV	p_o	K_B^* mM
CCh	2	−85	0.52	2.2
		−135	0.38	1.2
CCh	5	−75	0.42	3.6
		−105	0.37	2.9
		−135	0.25	1.7
ACh	1	−45	0.88	7.5
		−125	0.55	1.2

The probability of being open, p_o, and the equilibrium constant for block, K_B^*, at different membrane potentials in ACh and CCh (in concentration x_B).The value of p_o was calculated from the main current as described in the text, and K_B^* was estimated as $x_B\, p_o/(1-p_o)$.

Experiments with acetylcholine and carbachol

At high concentrations of ACh and CCh (above roughly 5 μM and 50 μM, respectively) channel openings occurred in well defined clusters during which the probability of opening was high (Sakmann *et al.* 1980; Ogden & Colquhoun 1983). Two observations were made at ACh and CCh concentrations above 500 μM which suggest that the agonist may block the open channel. First, the amplitude of the single channel current was found to be reduced, and second, the noise associated with the open channel current was increased, when compared with amplitude and noise that were seen in experiments with low agonist concentrations at similar membrane potential and temperature.

Figure 5 shows single channel currents recorded with 2 mM CCh at −135 mV (upper record) and with 1 mM ACh at −125 mV (lower record). The horizontal bars at the end of each record indicate the current amplitude that would be expected under similar conditions with low agonist concentration; the mean open channel

current level is clearly considerably lower than this expected level. Furthermore, the noise about the open channel level is obviously very much greater than that while the channel is shut, whereas at low agonist concentrations the noise is increased only slightly when the channel is open. These observations could be explained if the agonists produced very brief channel blockages, and reduced the open channel lifetime considerably, so that both openings and blockages were usually sufficiently brief that the limited frequency response of the recording apparatus prevented the recorded signal from reaching full amplitude. (Under the conditions of figure 5 rectangular pulses of 200 μs duration reached 95% of full amplitude.)

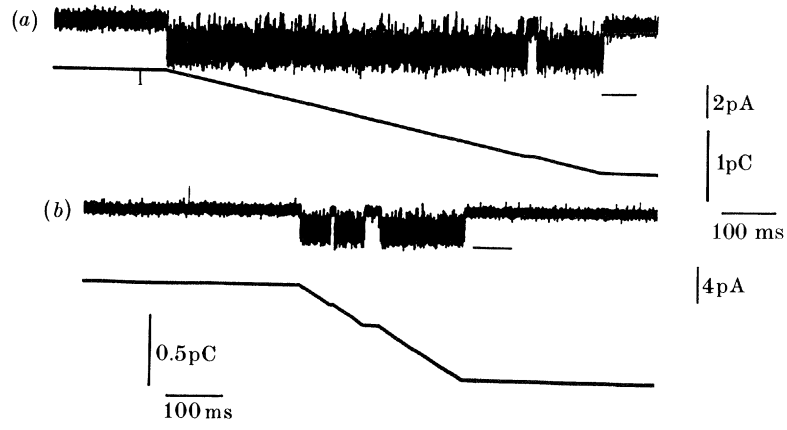

FIGURE 5. Single channel currents at high CCh and ACh concentrations. (*a*) Upper trace shows cluster of openings recorded with 2 mM CCh in the pipette. Calibration bar 2 pA. Potential −135 mV. Temperature 12 °C. Low pass filter 4 kHz (−3 dB, eight pole Bessel). Lower trace shows output of analogue integrator (τ = 10 s). Calibration bars 1 pC, 100 ms. (*b*) Upper trace shows cluster in 1 mM ACh. Potential −125 mV. Temperature 12 °C. Calibration bar 4 pA. Low pass filter 4 kHz (−3 dB, eight pole Bessel). Lower trace: integrated record, calibration bar 0.5 pC, 100 ms. Horizontal bars at the end of each cluster show the open current level expected for a channel conductance of 30 pS and a reversal potential of 0 mV.

Two sorts of measurement were made on these data. The extent of block at equilibrium was estimated from the reduction in mean current amplitude, and the rate of block was estimated from the characteristics of the excess open channel noise.

Equilibrium channel block

The mean current during a cluster of openings was estimated by integrating the current signal to obtain the total charge passed, and then dividing this by the length of the cluster. The integration was done either with an analogue integrator (with a time constant of 10 s), as illustrated in the lower traces in each record in figure 5, or by numerical integration of the digitized record (see Neher 1983). It may be noted that this procedure gives estimates of the mean currents which are unaffected by low pass filtering of the current record. In some cases, there is, of course, ambiguity about the demarcation of the start and end of a cluster of openings, that is, about what shut periods should be included within the cluster.

Nevertheless it was found that the slope of the integrator trace was constant throughout most of a cluster (see figure 5), and that reasonably reproducible results were obtained from one cluster to another.

If we now make the assumption (as was done for SubCh, above) that the channel would have been open for almost all of the time during a cluster if it were not for channel block (Ogden & Colquhoun 1983; Colquhoun & Sakmann 1985), then values for the probability of a channel being open (p_o) in the presence of block can be made by dividing the mean current, found as above, by the full current amplitude obtained with low concentrations of agonist at similar potential and temperature. Low and high concentration data were necessarily obtained from different membrane patches; in some cases these were from the same endplate, in others they were from different fibres, but this is not likely to be a serious problem because a high degree of uniformity has been found in the conductance and reversal potential of nicotinic ion channels at the frog neuromuscular junction (Gardner *et al.* 1984; Colquhoun & Sakmann 1983).

As the concentration of CCh was increased above 500 μM p_o declined, for example, from a mean maximum value of 0.81 for 500 μM CCh, to 0.25 in 5 mM CCh (at −130 mV and −135 mV respectively). Similarly with ACh p_o declined from 0.91 with 100 μM ACh to 0.55 with 1 mM (at −125 mV). Mean values of p_o obtained with concentrations of 1 mM and greater at different potentials are summarized in table 2.

Estimates were made of the equilibrium constants (K_B^*) for the interaction of ACh and CCh with the open channel from the decline of p_o at high concentration in a similar way to that described for SubCh above. Figure 4 shows Hill plots of the decline of p_o at high concentrations for ACh (solid circles) and CCh (open circles). The results gave estimated equilibrium constants of $K_B^* = 1.2$ mM for ACh (between −100 and −125 mV) and $K_B^* = 1.6$ mM for CCh (between −120 and −140 mV). The slopes of the plots were 0.94 ± 0.04 for ACh, and 0.96 ± 0.21 for CCh; these are compatible with the unit slope predicted by the simple block mechanism. Values of K_B^* were found to decrease (that is, affinity increased) with membrane hyperpolarization in the range −75 mV to −150 mV, with an e-fold change for about 70 mV. This is expected, and usually observed, for a wide range of positively charged channel-blocking molecules which presumably bind inside the open channel, within the membrane electric field.

The rate of channel block

It is possible to make estimates of the rate of the open channel blocking and unblocking reactions from the increase in the amount of noise that occurs when the channel is 'open' at high ACh and CCh concentrations. To measure this increase, sections of data in which the channel appeared to be open (though with reduced amplitude) for most of the time were low-pass filtered at 4 kHz or 8 kHz (−3 dB, 8 pole Butterworth filter) and digitized at 8192 Hz or 16384 Hz, respectively. The same procedure was followed for sections of the record throughout which the channel appeared to be closed. The variance about the mean of 512 point samples was calculated, and averaged over 20–48 such samples. The noise variance while the channel was open was 2.5–9 times the background level.

Spectral density functions were calculated for open channel and for background

noise; an example is shown in figure 6*a*, for 1 mM ACh at −110 mV. The variance is seen to be increased above background over the whole frequency range (up to 8 kHz here). The difference between these spectra, that is, the spectrum of the excess noise when the channel is open for most of the time, is shown in figure 6*b*. The net excess variance is summarized for ACh and CCh in column 3 of table 3 (the values have been corrected as described below).

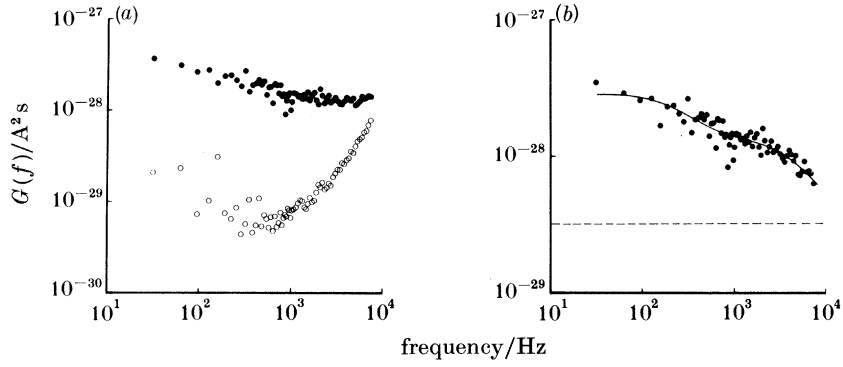

FIGURE 6. Spectral density of current noise in 1 mM ACh at −110 mV. (*a*) 512 point spectra calculated from current recorded during (●) and between (○) clusters in 1 mM ACh. Sampling frequency 16384 Hz, low pass filter 8 kHz (−3 dB, eight pole Butterworth). (*b*). Net spectrum of noise during cluster obtained by subtraction of data in (*a*). Fitted by sum of two Lorentzian curves and a constant, low amplitude component (indicated by the dotted line). The fitted solid curve has the following parameters $G_1(0) = 0.16 \times 10^{-27}$ A² s, $f_1 = 276$ Hz, $G_2(0) = 0.99 \times 10^{-28}$ A² s, $f_2 = 5373$ Hz, $G_3(0) = 0.31 \times 10^{-28}$ A² s.

TABLE 3. THE RATE OF CHANNEL BLOCK BY ACH AND CCH

agonist and concentration	membrane potential	mean current	observed variance	predicted variance	f_c	$k^*_{+B} \times 10^{-7}$	$k^*_{-B} \times 10^{-4}$
mM	mV	pA	pA²	pA²	kHz	M⁻¹ s⁻¹	s⁻¹
ACh (1 mM)	−110	−2.34	0.83	2.2	12.4	2.3	5.5
	−125	−1.73	0.91	3.5	18.5	6.3	5.3
	−125	−1.91	0.97	3.5	17.5	3.1	5.5
	−125	−2.40	1.0	3.2	14.6	3.3	5.9
mean ± s.e.	—	—	—	—	—	3.7 ± 0.9	5.6 ± 0.13
CCh (2 mM)	−135	−1.59	0.32	4.0	66.0	12.7	16.1
	−85	−1.30	0.31	1.6	31.8	4.9	10.2
CCh (5 mM)	−140	−0.98	0.13	3.2	64.6	6.2	9.4
	−140	−0.98	0.12	3.2	70.2	6.8	10.3
	−140	−0.94	0.14	3.1	62.4	6.1	8.8
mean ± s.e.	—	—	—	—	—	7.3 ± 1.4	11.0 ± 1.3

The rate of channel block as estimated from the excess open channel noise at high agonist concentration. Column 3 shows the mean current amplitude during a cluster of openings. Column 4 shows the observed excess variance while the channel is open compared with when it is shut, after correction by subtraction of the low frequency component of the variance (see text). Column 5 shows the variance predicted from the mean current (see equation (1)). Column 6 shows the half-power frequency calculated for the high frequency component. The last two columns give the calculated association and dissociation rate constants for block of the open channel (see text and equation (2)). Temperature 10–12 °C. Recording bandwidth 8 kHz (rows 1–6) or 4 kHz (rows 7–9) (−3 dB, eight-pole Butterworth filter).

If we suppose that the excess variance results only from brief complete shuttings of an open channel, then the magnitude of the variance for a single channel would be expected, from the binomial distribution, to be

$$\begin{aligned} \text{var}\,(i) &= i^2 p_o(1-p_o) \\ &= m_i(i-m_i) \end{aligned} \tag{1}$$

where i is the full amplitude of the single channel current (estimated from experiments with low concentrations), p_o is the probability of being open (estimated from the mean current as described above), and $m_i = ip_o$ is the mean current. The variances predicted in this way are tabulated in column 4 of table 3. Comparison of these with the observed excess variance in column 3 shows that only 10–30 % of the predicted variance was recorded. This might be explained if much of the excess variance were at frequencies greater than the recording bandwidth (usually 8 kHz).

The observed net spectrum (figure 6*b*) contained low and high frequency components. Under conditions where most interruptions of openings are caused by brief blockages it would be expected that the spectral density would consist predominantly of a single Lorentzian component with a time constant, τ, and half power frequency, f_c, given approximately by

$$\begin{aligned} 1/\tau = 2\pi f_c &= k^*_{-B} + k^*_{+B} x_B \\ &= k^*_{-B}(1 + x_b/K^*_B), \end{aligned} \tag{2}$$

where k^*_{-B} and k^*_{+B} are the dissociation and association rate constants for blockage, $K^*_B = k^*_{-B}/k^*_{+B}$ is the equilibrium constant, and x_B is the blocker concentration. These blockages are expected to be brief so the half-power frequency $f_c = 1/2\pi\tau$ should be high. There should also be components (of much smaller amplitude) with half-power frequencies that are related to the channel opening rate; these are also expected to be high at high agonist concentrations.

In fact the net spectrum usually showed evidence of a rather low frequency component, with small amplitude, as well as a high frequency component (see figure 6). This low frequency component (τ = 0.8–3 ms in ACh, τ = 0.2–0.4 ms in CCh) is not expected either in the presence or the absence of channel block. Its origin is obscure at present (see Discussion) but it is unlikely to be related to channel block, so the variance associated with this component (normally less than 25 % of the observed total) was subtracted from the observed variance to give a better estimate of the variance associated with channel block. Values corrected in this way are given in column 3 of table 3.

The predominant high frequency component of the spectrum appeared to roll-off at 4–6 kHz in 1 mM ACh and at 5–7 kHz in 2 mM CCh. These values are close to those expected from the frequency response of the system, which had a half-power frequency of 7.3 kHz for white noise (8 kHz filter).

The ratio of the predicted channel block variance in column 4 of table 3, to that observed in column 3, was used to estimate the half-power frequency, f_c of the Lorentzian curve that would give rise to this ratio when low pass-filtered as in the experiment. The method used for this calculation is described in Appendix 1. The

values of f_c so estimated are given in column 5 of table 3. They ranged from 12.4 to 18.5 kHz for 1 mM ACh (at -110 to -125 mV), and from 62 to 70 kHz with CCh. If this value of f_c is interpreted according to equation (2), then, since we already have an estimate of K_B^* (see above), an estimate can be made of k_{-B}^*, and hence of $k_{+B}^* = k_{-B}^*/K_B^*$.

The values for the rate constants so found are given in columns 6 and 7 of table 3. The average values for ACh were $k_{+B}^* = (3.7 \pm 0.9) \times 10^7$ M^{-1} s^{-1} ($n = 4$) for the blocking rate constant, and $k_{-B}^* = (5.6 \pm 0.1) \times 10^4$ s^{-1} ($n = 4$) for the unblocking rate constant (at -110 mV to -125 mV). The latter value corresponds to a mean blockage duration of 18 μs. For CCh (at -135 mV to -140 mV) the average blocking rate constant was $(7.3 \pm 1.4) \pm 10^7$ M^{-1} s^{-1} ($n = 5$), and the average unblocking rate constant was $(11.0 \pm 1.3) \times 10^4$ s^{-1} ($n = 5$) which corresponds to a mean blockage duration of 9 μs.

Discussion

Evidence has been presented that SubCh, CCh and the transmitter itself, ACh, can block the ion channels which they open at the neuromuscular junction. Knowledge of the extent and rate of block is essential for investigations into the mode of action of agonists at the nicotinic receptor because channel block must inevitably interfere with such investigations. It is also of interest to investigate the extent to which simple plugging and unplugging of the ion channel can account for the experimental results because recent work has shown that a number of channel blocking molecules behave in a more complex way than had previously been suspected (see, for example, Neher 1983; Ogden *et al.* 1981).

Block by SubCh

SubCh appeared to produce discrete blockages of about 5 ms average duration at -105 mV. Observations made on nicotinic ion channels of BC3H1 cells by Sine & Steinbach (1984) were qualitatively similar, but the affinity of SubCh for open endplate channels found here appears to be about 30 times higher than that found in BC3H1 cells. This is largely a result of the slower dissociation rate that we find here. At a membrane potential of -105 mV, and at 10 °C, we find an association rate constant of $k_{+B}^* = 3.9 \times 10^7$ M^{-1} s^{-1}, only slightly faster than the value of 1.1×10^7 M^{-1} s^{-1} inferred for similar conditions from the results of Sine & Steinbach (1984). However, the dissociation rate constant of 221 s^{-1} (mean blockage length of 4.5 ms) is much slower than theirs (1850 s^{-1}, mean blockage length 0.54 ms) and accordingly our equilibrium constant (5.7 μM) is much smaller than theirs (170 μM).

It is predicted for a simple channel blocker that the total open time produced by a single activation by agonist will be independent of blocker concentration (Colquhoun & Hawkes 1982, 1983; Neher 1983; Appendix 2). This prediction has been found to be untrue in the case of the quaternary lignocaine derivative QX222 (Neher 1983) and benzocaine (Ogden *et al.* 1981, 1985); on the basis of this, and other, evidence it has been suggested that these agents may not only block open channels, but may induce long-lived shut-blocked (and, perhaps, desensitized) states, or have a mechanism of action in which the blocked channel can return to

the resting state without re-opening. In the present experiments most of the SubCh concentrations were such that channel activations were frequent, so it was not possible to distinguish unambiguously between the end of one activation and the beginning of the next. The total open time per activation could not therefore be measured in these experiments. Instead we have plotted (figure 3) the mean number of blockages (4–5 ms gaps) per unit open time against blocker concentration (the 'blockage frequency' plot). It is shown in Appendix 2 that this plot can give similar information to that which would be found from measurements of the total open time per activation, but it does not require that activations be distinguishable from one another; it can be inferred from the distributions of all shut times and of all open times, as long as the former contains a component that can be identified clearly as blockages. For a simple channel blocker it is predicted that the 'blockage frequency' plot will have a slope equal to the association rate constant, k^*_{+B}, for open channel block, the same slope as that for the plot of reciprocal mean open time against blocker concentration. For more complex modes of block (see Appendix 2) the slope of the former plot should be less than that of the latter. In fact it was observed that 'blockage frequency' plot was close to a straight line and that its slope was very close to that found for the reciprocal mean open time, as would be expected for simple channel block. It is shown in Appendix 2 that this observation implies that it is unlikely that there exist long-lived shut-blocked state of the channel; for example, it is unlikely that the channel can shut around, and trap, the agonist in the way observed for some antagonists in ganglionic nicotinic channels (Gurney & Rang 1984; see also Lingle 1983*a*, *b*). According to some simplified models (for example, (A 2.1)), this observation should also rule out the existence of a direct route from the blocked state or states to the resting state which would allow recovery from block without re-opening of the channel. However, the consideration of more realistic mechanisms given in Appendix 2 shows that these methods of analysis are not likely to be very sensitive to presence or absence of such routes.

The distribution of shut times in SubCh (table 1) shows, in addition to the 4–5 ms gaps, a component of 25–50 μs gaps which decreases in relative proportion as SubCh concentration is increased. Colquhoun & Sakmann (1981, 1985) reported brief gaps of this duration at low concentrations of SubCh. In the present data the frequency of such brief gaps per unit open time can be calculated from the results in table 1 as $k^*_{+B}\, x_B$ multiplied by the ratio of area for brief gaps to the area for blockage gaps, the areas being those under the fitted distribution of shut time durations. This calculation gives 0.48 ± 0.1 (s.e., $n = 5$) brief gaps per millisecond of open time, with no consistent dependence on agonist concentration, a result that agrees closely with the value of 0.47 per millisecond reported by Colquhoun & Sakmann (1985) under similar conditions. The effect of these brief gaps on the analysis of channel block mechanisms is considered in Appendix 2.

Block by ACh and CCh

Measurements of the equilibrium constant, K^*_B, for open channel block based on the reduction of mean current during periods of high activity gave $K^*_B = 1.2$ mM for ACh (at about -110 mV) and $K^*_B = 1.6$ mM for CCh (at about -130 mV). These

values, unlike those for SubCh, are very similar to those found by Sine & Steinbach (1984) at similar membrane potentials, namely, 1.5 mM for ACh and 1.6 mM for CCh (though the latter value was at a higher temperature, 21 °C). In both studies K_B^* decreased with hyperpolarization as expected for a charged blocker. Over the range −75 mV to −150 mV we found an average of about 70 mV for an e-fold change in K_B^*, whereas Sine & Steinbach found 31 mV. This difference may well be attributable to the fact, demonstrated by Sine & Steinbach (1984), that the voltage-dependence of K_B^* becomes less at more hyperpolarized membrane potentials, presumably because ACh and CCh can permeate through the channel and dissociate inwards towards the cytoplasm, an effect that will become more predominant as the membrane is hyperpolarized.

The results found here do not allow any conclusions to be drawn concerning the possibility that blocked shut states might exist or that there may be routes for direct shutting of blocked channels.

Estimates have been made of the rates of association and dissociation of ACh and CCh from the open channel, from measurements of the excess noise during a cluster of openings. The association rate constants found (3.7×10^7 M^{-1} s^{-1} for ACh, and 7.3×10^7 M^{-1} s^{-1} for CCh) are in the usual range of values for many bimolecular reactions, which lends some plausibility to our calculations. Furthermore the inferred mean length of a blockage for CCh, 9 μs, is quite close to the value of 13 μs that was found by direct observation of brief gaps during CCh-induced channel openings by Colquhoun & Sakmann (1985). They found that these brief gaps (unlike those seen with other agonists) increased in frequency with increasing CCh concentration and could be accounted for by open channel block with an association rate constant of 4.2×10^7 M^{-1} s^{-1} and an equilibrium constant of 1.8 mM (at −130 mV), values that are very close to those inferred by the method used here.

The present results suggest that the mean length of a blockage produced by ACh is about 18 μs and this conclusion was borne out by direct measurement of single channel currents which showed a prominent component of gaps of 19–25 μs which increased, as a proportion of all gaps, in the range 5–200 μM ACh, as expected for blockage gaps. The mean duration of 18 μs is rather close to the length of the brief gaps observed in ACh-induced channel openings by Colquhoun & Sakmann (1983, 1985) at very low agonist concentrations (up to 500 nM); however, the frequency of 20 μs gaps observed by them was not dependent on agonist concentration, and so the gaps were presumably not a result of channel block. The association rate constant found here suggests that at the highest ACh concentration used by Colquhoun & Sakmann (1985), namely 500 nM, there should be about 0.018 blockages per millisecond of open time, whereas 0.46 gaps per millisecond were observed by them. Therefore it seems that blockages and spontaneous brief gaps have very similar mean durations, but quite different mechanisms, in the case of ACh.

The spectral density of the excess open channel noise (see figure 6) showed a slow component which was assumed to be unconnected with channel block. The source of this component is not known but it may be the same as that observed by Sigworth (1982) at low agonist concentrations who suggested that it might result

from thermal fluctuations in the protein conformation of the open channel. It could also result, at least in part, from inclusion in the data of some longer shut periods that were not produced by channel blockages.

In a recent paper Yellen (1984) has proposed a different method for extraction of blocking and unblocking rates from the excess noise while the channel is open. He fits the amplitude distribution of the observations while the channel is open with a theoretical relationship based on the same assumption as ours, namely, that most of the noise arises from brief but complete blockages of the open channel. Both methods suffer from the need to select, rather arbitrarily, what sections of the record are to be used for analysis. However Yellen's method has the following disadvantages. (i) The spectral characteristics of the excess noise are ignored so there is no opportunity to correct for components of the noise that are not connected with channel block, whereas such correction (for example, that for the low frequency component in our data) are relatively easy in the frequency domain. (ii) His method has an analytical solution only for a first order filter, so the filters actually used must be corrected-for empirically; on the other hand any filter can be incorporated into the analysis in the frequency domain (see Appendix 1). (iii) In the amplitude distribution analysis the effect of background noise must be treated by convolution of an idealized version of the background amplitude distribution with the predicted probability density whereas in the frequency domain the observed background spectral density can simply be subtracted from the 'open channel' spectral density.

Thus our method of analysis, based on the spectral density of the excess 'open' channel noise appears to have several advantages compared with the amplitude distribution analysis.

It is conceivable that some channel block by ACh could occur during synaptic transmission. The concentration of ACh in the synaptic cleft may, very transiently, reach concentrations as high as 1 mM. The time constant for equilibration of ACh block with channels that are already open would be $1/(k^*_{+B}\, x_B + k^*_{-B})$, that is, only about 10 μs at a concentration of 1 mM and a membrane potential of −90 mV, and the equilibrium extent of channel block would be about 40%. However, as soon as the postsynaptic membrane depolarized the rate of dissociation of blocker would become even faster and, furthermore, the agonist concentration in the cleft falls rapidly (Mableby & Stevens 1972) so there would be little reassociation. Therefore, it is probable that any transient initial block would very rapidly disappear. Thus it seems unlikely that channel block by ACh has any great physiological consequences although it is clearly very important to allow for such block in experiments that are designed to study channel behaviour at high ACh concentrations.

We thank Dr J. H. Steinbach for helpful discussion and Professor B. L. Ginsborg and Professor D. H. Michael for help with Appendix 1. This work was supported by the M.R.C.

Appendix 1

The area under a filtered Lorentzian spectrum

To estimate the rate of ACh block by the method used in the text we need to know the reduction in variance that will be produced by low pass filtering of a noisy signal with a Lorentzian spectral density function. Define R as the ratio of the variance (area of spectrum) of the unfiltered signal to that of the filtered signal. In practice the former was estimated from equation (1) and the latter was estimated as the corrected observed variance, to obtain an experimental value for R. Also define f_f as the (known) half power frequency of the filter, and f_c as the (unknown) half power frequency of the unfiltered Lorentzian.

If the filter has a frequency response function $B(f)$ then

$$R = \frac{\int_0^\infty [1+(f/f_c)^2]^{-1}\,df}{\int_0^\infty |B(f)|^2\,[1+(f/f_c)^2]^{-1}\,df}. \tag{A 1.1}$$

This expression can be evaluated for various filter types. The resulting equations can be solved to obtain a value of f_c that corresponds to the observed value of R.

Gaussian filter

A Gaussian filter (see Colquhoun & Sigworth 1983) with cut-off frequency f_f has a frequency response function

$$B(f) = \exp\,[-0.5\,\ln(2)\,(f/f_f)^2],$$

so evaluation of (A 1.1) gives

$$\begin{aligned} R &= e^{-z^2}/[1-\mathrm{erf}(z)] \\ &\approx \pi^{0.5}\,z\left[1-\frac{1}{2z^2}+\frac{3}{(2z^2)^2}-\frac{15}{(2z^2)^3}+\ldots\right]^{-1}, \end{aligned} \tag{A 1.2}$$

where

$$z = (\ln 2)^{0.5}\,(f_c/f_f)$$

The latter approximate form is suitable for numerical evaluation when z is large.

Perfect filter

For a filter that passes all frequencies below f_f but no frequencies above f_f (square cut-off) we have

$$R = (\pi/2)/\tan^{-1}(f_f/f_c). \tag{A 1.3}$$

This can be solved directly for f_c, giving

$$f_c = f_f/\tan(\pi/2R). \tag{A 1.4}$$

Butterworth filter

An n pole Butterworth filter has frequency response function

$$B(f) = 1/[1+(f/f_f)^{2n}]^{0.5} \tag{A 1.5}$$

To evaluate the denominator of (A 1.1) it will be necessary to present first a general definite integral (derived by Professor D. H. Michael and Professor B. L. Ginsborg). If m and n are positive integers (for example, $m = 1$ for a Lorentzian spectrum and n = number of poles for Butterworth filter) then

$$\int_0^\infty \frac{dx}{[1+(x/a)^{2m}][1+(x/b)^{2n}]} = F(m,n,a,b)+F(n,m,b,a), \qquad \text{(A 1.6)}$$

where the function $F(j, k, y, z)$ is defined as follows.

If j is even then

$$F(j,k,y,z) = (\pi y/j)\sum_{r=0}^{r_1} G(r,j,k,y,z) \qquad \text{(A 1.7)}$$

where $r_1 = (j/2)-1$.

If j is odd then

$$F(j,k,y,z) = (\pi y/j)\left[\frac{1}{2[1+(-1)^k(y/z)^{2k}]}+\sum_{r=0}^{r_2} G(r,j,k,y,z)\right] \qquad \text{(A 1.8)}$$

where $r_2 = (j/2)-(3/2)$. Notice that the summation term in (A 1.8) vanishes when $j = 1$.

In both (A 1.7) and (A 1.8) the function G is defined as

$$G(r,j,k,y,z) = \frac{\sin[(2r+1)\pi/2j]-(y/z)^{2k}\sin[(2r+1)(2k-1)\pi/2j]}{1+(y^2/z^2)^{2k}+2(y/z)^{2k}\cos[(2r+1)\pi k/j]}. \qquad \text{(A 1.9)}$$

The general result in (A 1.6) to (A 1.9), with $m = 1$ and $n = 8$, allows evaluation of (A 1.1) for an eight-pole Butterworth filter. The result is

$$R = \left[\frac{1}{1+(f_c/f_f)^{16}}+\frac{1}{4}\left(\frac{f_f}{f_c}\right)\left[1-\left(\frac{f_f}{f_c}\right)^2\right]\sum_{r=0}^{r=3}\left(\frac{\sin[(2r+1)\pi/16]}{1+(f_f/f_c)^4+2(f_f/f_c)^2\cos[(2r+1)\pi/8]}\right)\right]^{-1}. \qquad \text{(A 1.10)}$$

The case of heavy filtering

When f_c is large compared with the filter cut-off frequency a large part of the variance of the Lorentzian spectrum will be lost by filtering, and the following much simpler forms will be good approximations.

For the Gaussian filter (A 1.2) gives

$$R \approx (\pi \ln 2)^{0.5}(f_c/f_f) = 1.476\,(f_c/f_f). \qquad \text{(A 1.11)}$$

This is accurate to better than 5% if $R > 3.5$.

For the perfect filter (A 1.3) gives

$$R \approx (\pi/2)\,(f_c/f_f) = 1.571\,(f_c/f_f). \qquad \text{(A 1.12)}$$

This is accurate to better than 5% if $R > 2.5$.

And for the eight-pole Butterworth filter (A 1.10) gives

$$R \approx \frac{16\sin(\pi/16)}{2}(f_c/f_f) = 1.561\,(f_c/f_f). \qquad \text{(A 1.13)}$$

This is accurate to better than 5% if $R > 2.5$.

Thus, for practical purposes, the above filter types do not differ greatly in the limit (A 1.11) to (A 1.13) or, indeed, over most of their range.

Appendix 2

Characteristics of channel block that is not selective for the open state

We shall now consider how inferences might be made from single channel measurements concerning the extent to which simple plugging and unplugging of the open channel can explain experimental results. In particular we shall discuss the characteristics of the new 'blockage frequency' plot that was introduced in figure 3.

A simple case

Consider the mechanism shown in (2.1), in which a direct route from blocked to shut states is shown.

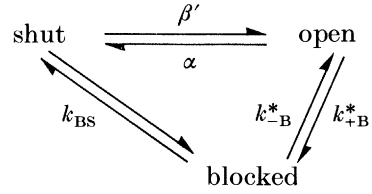

(A 2.1)

This was used by Ruff (1977). It is physically unrealistic in that there must actually be at least two steps in the shut-blocked pathway. Also this model assumes that agonist binding is very fast compared with the other reactions, as does the four state model invoked by Adams (1977) in which open-blocked and shut-blocked states are distinguished.

Blocking and unblocking will cause activations to appear as bursts of openings with a mean gap (blockage) length of $1/(k^*_{-B}+k_{BS})$, which becomes simply $1/k^*_{-B}$ if the shut-blocked pathway does not exist. In the latter case the mechanism will be referred to as simple channel block.

The probability (π_{BS} say) that a blocked channel will escape to the resting shut state, rather than unblocking to return to the open state is

$$\pi_{BS} = \frac{k_{BS}}{k^*_{-B}+k_{BS}}. \tag{A 2.2}$$

and the probability (π_{BO}) that it will return to the open state is thus

$$\pi_{BO} = 1-\pi_{BS}. \tag{A 2.3}$$

If the blocked channel cannot shut directly then $\pi_{BS} = 0, \pi_{BO} = 1$. The mean length of a single opening in the absence of the blocker is

$$m_o = 1/\alpha, \tag{A 2.4}$$

whereas in the presence of blocker (in concentration x_B) it becomes

$$m_{ob} = 1/(\alpha+k^*_{+B}x_B), \tag{A 2.5}$$

regardless of whether the blocked channel can shut directly. However, the mean open time per burst,

$$m_t = \frac{m_o}{1 + m_o k^*_{+B} x_B \pi_{BS}}, \tag{A 2.6}$$

will be reduced below the value ($m_0 = 1/\alpha$) expected for a simple blocker if direct shutting is possible ($\pi_{BS} > 0$). And the mean number of openings per burst,

$$n_b = \frac{1 + m_o k^*_{+B} x_B}{1 + m_o k^*_{+B} x_B \pi_{BS}}, \tag{A 2.7}$$

will likewise be reduced, by the same factor, from its value for a simple blocker, namely, $1 + m_o k^*_{+B} x_B = 1 + (k^*_{+B} x_B/\alpha)$. For a simple blocker n_b should increase linearly with x_B (slope k^*_{+B}/α), but (A 2.7) increases less than linearly and should saturate at $1/\pi_{BS}$.

When it is not possible to distinguish individual bursts (for example, because of the fast activation rate as in the present case) then it may still be possible to estimate the number of blockages per unit open time, as long as a component of the distribution of all shut times can be identified as representing channel blockages. (Inference of the number and duration of blockages from this distribution is itself an approximation, but is likely to be a good one if other components of the distribution have time constants that are well separated from the mean blockage duration.) For the mechanism in (A 2.1) the mean number of blockages per unit open time ('blockage frequency') will be

$$\begin{aligned} f = (n_b - 1)/m_t &= k^*_{+B} x_B (1 - \pi_{BS}) \\ &= k^*_{+B} x_B \pi_{BO} \end{aligned} \tag{A 2.8}$$

so a plot of f against blocker concentration (as in figure 3) should have a slope of $k^*_{+B}(1 - \pi_{BS})$. It will be reduced below its value for a simple blocker (namely k^*_{+B}) by a factor that, like the reduction in m_t and n_b, depends on the extent to which π_{BS} is greater than zero.

A more realistic analysis

The simple example above suggests that reduction of the open time per burst, etc., will be seen only if blocked channels can shut without re-opening. Analysis of more realistic mechanisms shows that this is not so.

Some mechanisms

It is doubtful whether agonist binding can be considered very rapid in the frog (Colquhoun & Hawkes 1977; Colquhoun & Sakmann 1981, 1983, 1985). Given that two agonist molecules must be bound for effective channel opening, the scheme shown in figure 7*a* must be considered. Some simplified versions of it are shown in figure 7*b*, *c* and *d*. It has been suggested that rapid oscillations between the open state and states 2 and 3 may cause very brief shut periods (mean length about 40 μs in the case of SubCh here) so channel openings normally occur as bursts. Sojourns in the blocked states will cause, in the case of most blockers, longer shut periods to appear (with a mean length of about 5 ms in the case of SubCh, which

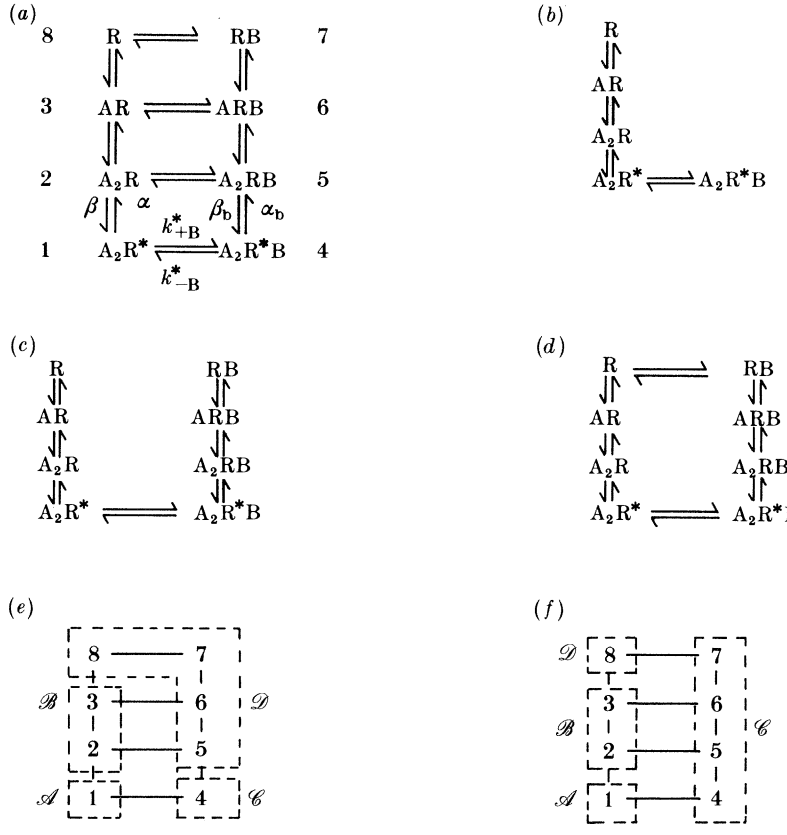

FIGURE 7. Some mechanisms for channel block. The receptor–channel is represented as R, the agonist as A and the blocker as B. The asterisk represents the open conformation of the channel (but the blocked form A_2R^*B is assumed to be non-conducting). (*a*) General scheme for block of both open and shut states, with the numbering of the states and some of the rate constants indicated. (*b*) Simple channel block. (*c*) Block of shut states (for example, trapping block) with obligatory return from blockage via the open state. (*d*) As in (*c*) but with a route for return to the resting state without re-opening of the channel. No direct communication between $\mathscr{B}$ and $\mathscr{C}$ states (as is also the case in (*b*) and (*c*)). (*e*) Allocation of states in (*a*) to subsets (script letters, see text) when the shut-blocked states have got a long lifetime so that entry into them terminates a cluster. (*f*) Allocation of states in (*a*) to subsets when the shut-blocked states have not got a long lifetime, and agonist concentration is low so state R only has got a long lifetime.

is of primary interest here). Thus a single activation of the channel by SubCh may be expected to produce a cluster of bursts of openings with average gaps of about 40 μs within a burst, and of 5 ms between bursts within a cluster. It should be noted that the word *cluster* is being used in this appendix in a different sense from that which is used in the rest of the paper, in which cluster refers to the much longer groups of openings, containing many individual activations, that are separated by long silent periods in desensitized states.

We shall consider the following cases. (i) Simple channel block, defined as a mechanism, like that in figure 7*b*, in which there is a single blocked-open state

which can communicate directly only with the open state, for example, a simple plugging and unplugging of the open channel. (ii) Cases in which the blocked channel can shut (perhaps with the agonist trapped inside it, as described by Gurney & Rang (1984)), but in which the blocked channel can still get back to the resting state only by re-opening. An example with several shut-blocked states is shown in figure 7*c*. (iii) Cases in which a route exists for shutting of the blocked channel without re-opening, but in which the blocked states cannot communicate directly with the gap-within-burst states. An example is shown in figure 7*d*.

The analysis

We shall use a method for the analysis of clusters of bursts that was described by Colquhoun & Hawkes (1982), to which reference should be made for further details of the methods and notation.

Let $\mathscr{A}$ denote the subset of open states (state 1 in figure 7); $\mathscr{B}$ denotes the subset of very short-lived shut states (states 2 and 3 in figure 7); $\mathscr{C}$ denotes the subset of blocked states that are responsible for the longer gaps within clusters; and $\mathscr{D}$ denotes the subset of very long-lived shut states, entry into which is interpreted as a gap between clusters (see figure 7*e*, *f*). We also define the subset $\mathscr{F}$ that includes both $\mathscr{B}$ and $\mathscr{C}$ states. Which states are allocated to $\mathscr{C}$ and $\mathscr{D}$ will depend on the agonist concentration and the life of shut-blocked states. For each mechanism it will be important to consider whether the lifetime in shut-blocked states is long (so entry into these states terminates a cluster and these states are therefore allocated to subset $\mathscr{D}$), or whether the time spent in shut-blocked states is short (so entry into *any* blocked state produces a relatively brief shut period within a cluster, and shut-blocked states are therefore allocated to subset $\mathscr{C}$). In the present case there is assumed to be only one open state so the results given will all be the special cases of those presented by Colquhoun & Hawkes (1982) for $k_{\mathscr{A}} = 1$.

Single openings and bursts in the presence and absence of block

The following results apply to all the block mechanisms in figure 7, regardless of shutting route. The mean length of a single opening in the absence and presence of blocker are still given by (A 2.4) and (A 2.5) exactly as before, for all the mechanisms in figure 7. However, in the present context, the analogue of a single opening in the simple example above is a single burst of openings separated by very brief shut periods in $\mathscr{B}$. The total open time per burst in the absence of channel block, $m_0' = 1/\alpha_{\text{eff}}$ say, is given (for example, from equations 3.26, A 1.9 and 5.4 from Colquhoun & Hawkes (1982)) by

$$m_0' = 1/\alpha_{\text{eff}} = 1/(\boldsymbol{Q}_{\mathscr{A}\mathscr{D}} + \boldsymbol{Q}_{\mathscr{A}\mathscr{B}}\boldsymbol{G}_{\mathscr{B}\mathscr{D}})\,\boldsymbol{u}_{\mathscr{D}}. \qquad \text{(A 2.9)}$$

In this result $\boldsymbol{Q}_{\mathscr{A}\mathscr{D}}$, etc., represent submatrices of the matrix of transition rates, and $\boldsymbol{G}_{\mathscr{B}\mathscr{D}} = (-\boldsymbol{Q}_{\mathscr{B}\mathscr{B}})^{-1}\,\boldsymbol{Q}_{\mathscr{B}\mathscr{D}}$ represents the probability transition matrix for transitions from $\mathscr{B}$ states to $\mathscr{D}$ states (and similarly for other subscripts). The $\boldsymbol{G}$ matrices are generalizations, for the case when a subset contains more than one state, of the transition probabilities denoted as π above. The column vector $\boldsymbol{u}_{\mathscr{D}}$ has unit elements so postmultiplication by it sums the rows of the preceding matrix.

The symbol α_{eff} was introduced above because $m_0' = 1/\alpha_{\text{eff}}$ represents the *effective open channel lifetime* when the interruptions are very brief; it represents the same flow of charge as the burst, but will be slightly shorter than the burst because it does not include the time spent in the short gaps.

In the presence of channel block the effective open time (mean open time per burst) becomes, for *all* of the mechanisms in figure 7, regardless of shutting routes,

$$m'_{\text{ob}} = 1/(\alpha_{\text{eff}} + \boldsymbol{Q}_{\mathscr{A}\mathscr{C}}\boldsymbol{u}_{\mathscr{C}}). \tag{A 2.10}$$

This is exactly analogous with (A 2.5) because, if there is one route from $\mathscr{A}$ (open) to $\mathscr{C}$ (blocked) with rate constant $k^*_{+\text{B}}$, then

$$\boldsymbol{Q}_{\mathscr{A}\mathscr{C}}\boldsymbol{u}_{\mathscr{C}} = k^*_{+\text{B}}\,x_{\text{B}} \tag{A 2.11}$$

which is the transition rate from $\mathscr{A}$ to $\mathscr{C}$ when the blocker concentration is x_{B}.

Thus plots against blocker concentration of the reciprocal of either the individual opening length or the open time per burst (approximately equal to burst length) should both have a slope $k^*_{+\text{B}}$ regardless of the shutting route.

Analysis of clusters

When channel activations are sufficiently rare that clusters can clearly be distinguished from each other in the experimental record then the obvious measurements to make, in analogy with (A 2.6) and (A 2.7), are the mean open time per cluster, m_{t}, and the mean number of bursts per cluster, n_{b}. From equations 5.19, 5.35, A 2.4 and A 2.13 in Colquhoun & Hawkes (1982)

$$m_{\text{t}} = 1/[(-\boldsymbol{Q}_{\mathscr{A}\mathscr{A}})(1-\boldsymbol{G}_{\mathscr{A}\mathscr{F}}\boldsymbol{G}_{\mathscr{F}\mathscr{A}})], \tag{A 2.12}$$

$$n_{\text{b}} = (1-\boldsymbol{G}_{\mathscr{A}\mathscr{B}}\boldsymbol{G}_{\mathscr{B}\mathscr{A}})/(1-\boldsymbol{G}_{\mathscr{A}\mathscr{F}}\boldsymbol{G}_{\mathscr{F}\mathscr{A}}). \tag{A 2.13}$$

When activations are too frequent for this to be done it may nevertheless be possible, as above, to estimate the mean number of blockages per unit open time, the 'blockage frequency', f. From (A 2.12) and (A 2.13) this is

$$f = (n_{\text{b}}-1)/m_{\text{t}} = \boldsymbol{Q}_{\mathscr{A}\mathscr{F}}\boldsymbol{G}_{\mathscr{F}\mathscr{A}} - \boldsymbol{Q}_{\mathscr{A}\mathscr{B}}\boldsymbol{G}_{\mathscr{B}\mathscr{A}}. \tag{A 2.14}$$

These forms, although simple, involve the compound subset $\mathscr{F}$. To analyse the special cases in figure 7*b–d* it will be convenient to express the results in terms of $\mathscr{A}$, $\mathscr{B}$, and $\mathscr{C}$ only. This can be done by substitution (from A 2.12 and equations 5.5–5.7 in Colquhoun & Hawkes (1984)) of

$$\boldsymbol{G}_{\mathscr{A}\mathscr{F}}\boldsymbol{G}_{\mathscr{F}\mathscr{A}} = (\boldsymbol{G}_{\mathscr{A}\mathscr{C}}+\boldsymbol{G}_{\mathscr{A}\mathscr{B}}\boldsymbol{G}_{\mathscr{B}\mathscr{C}})(\boldsymbol{I}-\boldsymbol{G}_{\mathscr{C}\mathscr{B}}\boldsymbol{G}_{\mathscr{B}\mathscr{C}})^{-1}(\boldsymbol{G}_{\mathscr{C}\mathscr{A}}+\boldsymbol{G}_{\mathscr{C}\mathscr{B}}\boldsymbol{G}_{\mathscr{B}\mathscr{A}})+\boldsymbol{G}_{\mathscr{A}\mathscr{B}}\boldsymbol{G}_{\mathscr{B}\mathscr{A}}. \tag{A 2.15}$$

The above results will, of course, be useful in practice only to the extent that states are allocated to subsets sensibly. The conclusions that follow have been tested by numerical calculations. The 'blockage frequency' was calculated from (A 2.14), and also, as it would be experimentally, from the ratio of the area under the 'blockage' component in the distribution of all shut times to the mean length of a single opening (this method is, of course, independent of subset allocation);

these methods agreed well in all cases in which the blockage component could be clearly identified.

Some particular cases in which simple results can be obtained will now be considered.

The case of simple channel block

In this case there is no route from $\mathscr{C}$ to either $\mathscr{B}$ or $\mathscr{D}$ as in figure 7*b* (so $\boldsymbol{Q}_{\mathscr{C}\mathscr{B}} = \boldsymbol{Q}_{\mathscr{B}\mathscr{C}} = \mathbf{0}$, $\boldsymbol{Q}_{\mathscr{C}\mathscr{D}} = \boldsymbol{Q}_{\mathscr{D}\mathscr{C}} = \mathbf{0}$ and the blocked channel must re-open so $\boldsymbol{G}_{\mathscr{C}\mathscr{A}} = \boldsymbol{u}_{\mathscr{C}}$). Thus we get from (A 2.12) and (A 2.15)

$$m_t = m'_o = 1/\alpha_{eff} \tag{A 2.16}$$

so, as with scheme (A 2.1) (see A 2.6), the total open time per cluster is not changed by a simple channel blocker. Also

$$n_b = 1 + m'_o \boldsymbol{Q}_{\mathscr{A}\mathscr{C}} \boldsymbol{u}_{\mathscr{C}} \tag{A 2.17}$$

which, from (A 2.11), is exactly analogous with the result from scheme (A 2.1) (see A 2.7). It should increase linearly with blocker concentration. Finally the 'blockage frequency' becomes

$$f = \boldsymbol{Q}_{\mathscr{A}\mathscr{C}} \boldsymbol{u}_{\mathscr{C}}. \tag{A 2.18}$$

Thus, from (A 2.11), a plot of f against x_B will have a slope of k^*_{+B}.

The case when the lifetime of shut-blocked states is long

Suppose that entry into the shut-blocked state or states results in a shut period so long that it terminates a cluster, so that only $A_2R^* \rightleftharpoons A_2R^*B$ oscillations appear as 'blockages' in the record (for example, in the case of SubCh they would appear as 5 ms gaps between bursts within clusters). A similar analysis would obviously also apply if there were long-lived blocked-desensitized states distal to A_2R^*B. In this case the shut-blocked state or states (as well as the resting state, R at low agonist concentrations) must be allocated to subset $\mathscr{D}$ as shown in figure 7*e*. The 'blockages' would have a mean lifetime of $1/(k^*_{-B} + \alpha_b)$ (see figure 7 for definition of rate constants). As there is only one state in $\mathscr{C}$ we have

$$\boldsymbol{Q}_{\mathscr{A}\mathscr{C}} = k^*_{+B} x_B; \quad \boldsymbol{G}_{\mathscr{C}\mathscr{D}} \boldsymbol{u}_{\mathscr{D}} = \frac{\alpha_b}{k^*_{-B} + \alpha_b} = \pi_{\mathscr{C}\mathscr{D}}, \tag{A 2.19}$$

where $\pi_{\mathscr{C}\mathscr{D}}$ here has exactly the same meaning as π_{BS}, above (see 2.2).

Furthermore, there is, in this case, no direct route from $\mathscr{B}$ to $\mathscr{C}$ (see figure 7*e*), so $\boldsymbol{Q}_{\mathscr{B}\mathscr{C}} = \boldsymbol{Q}_{\mathscr{C}\mathscr{B}} = \mathbf{0}$; we therefore obtain, from (A 2.12)–(A 2.15), the mean open time per cluster as

$$m_t = \frac{m'_o}{1 + m'_o \boldsymbol{Q}_{\mathscr{A}\mathscr{C}} \boldsymbol{G}_{\mathscr{C}\mathscr{D}} \boldsymbol{u}_{\mathscr{D}}}. \tag{A 2.20}$$

This result, when taken with (A 2.19), is seen to be very similar to the result (A 2.6) found for scheme (A 2.1). The mean open time per cluster will be reduced below the value ($m'_0 = 1/\alpha_{eff}$) expected for a simple blocker if $\boldsymbol{G}_{\mathscr{C}\mathscr{D}} \neq \mathbf{0}$. The mean number of bursts per cluster is given by

$$n_b = \frac{1 + m'_o \boldsymbol{Q}_{\mathscr{A}\mathscr{C}} \boldsymbol{u}_{\mathscr{C}}}{1 + m'_o \boldsymbol{Q}_{\mathscr{A}\mathscr{C}} \boldsymbol{G}_{\mathscr{C}\mathscr{D}} \boldsymbol{u}_{\mathscr{D}}}, \tag{A 2.21}$$

which is exactly analogous with (A 2.7); it is reduced, by the same factor as in (2.20), below the value expected for a simple blocker (A 2.17), when $\boldsymbol{G}_{\mathscr{C}\mathscr{D}} \neq \boldsymbol{0}$.

The 'blockage frequency' becomes, when $\boldsymbol{Q}_{\mathscr{C}\mathscr{B}} = \boldsymbol{Q}_{\mathscr{B}\mathscr{C}} = \boldsymbol{0}$,

$$f = \boldsymbol{Q}_{\mathscr{A}\mathscr{C}} \boldsymbol{G}_{\mathscr{C}\mathscr{A}}$$
$$= \boldsymbol{Q}_{\mathscr{A}\mathscr{C}} (\boldsymbol{u}_{\mathscr{C}} - \boldsymbol{G}_{\mathscr{C}\mathscr{D}} \boldsymbol{u}_{\mathscr{D}}). \qquad \text{(A 2.22)}$$

This is exactly analogous with the result (A 2.8) found from scheme (A 2.1). It can be written as

$$f = k^*_{+\mathrm{B}} x_{\mathrm{B}} \text{ Prob (re-opens after being in } \mathscr{C} | \text{sojourn in } \mathscr{C} \text{ began by exit from the open state).} \qquad \text{(A 2.23)}$$

This shows that a plot of f against x_{B} (as in figure 3) will have a slope reduced below the value expected for a simple blocker, $k^*_{+\mathrm{B}}$, to an extent that depends on the relative rate at which the 'blockage' ($\mathscr{C}$) terminates by exit to $\mathscr{D}$ rather than to the open state ($\mathscr{A}$).

In the present case, in which there is only one blocked state in $\mathscr{C}$ (A 2.22) becomes, from (A 2.11) and (A 2.19),

$$f = k^*_{+\mathrm{B}} (1 - \pi_{\mathscr{C}\mathscr{D}}) x_{\mathrm{B}} = k^*_{+\mathrm{B}} \pi_{\mathscr{C}\mathscr{A}} x_{\mathrm{B}} = k^*_{+\mathrm{B}} \left(\frac{k^*_{-\mathrm{B}}}{k^*_{-\mathrm{B}} + \alpha_{\mathrm{b}}} \right) x_{\mathrm{B}} \qquad \text{(A 2.24)}$$

so the 'blockage frequency' plot will be linear with a slope reduced below $k^*_{+\mathrm{B}}$ by a factor that depends on the relative rates of blocker dissociation ($k^*_{-\mathrm{B}}$) and of shutting of the blocked channel (α_{b}).

The reason for this reduction can be put in another way. The distribution of the lifetime of sojourns in all blocked states will have more than one exponential component when there is more than one sort of blocked state. Under the above circumstances one component will have a short time constant that represents single sojourns in A_2R^*B followed by re-opening, and other component or components will have much longer time constant or constants that occur when states distal to A_2R^*B are reached; only the former may be recognizable as 'blockages' in the experimental record. If it *were* possible to recognize as such all sojourns in blocked states in the experimental records then none of the above measures would be reduced unless there was a route for shutting without re-opening (as in figure 7*a*, *d*, but not in figure 7*b*, *c*); otherwise the predictions are rather insensitive to the existence of such a route.

The case where the life time of shut-blocked states is short

If entry into *any* blocked states generates a shut period of sufficient brevity that it is counted as a 'blockage' gap within a cluster then all blocked states would be allocated to subset $\mathscr{C}$, as shown in figure 7*f*. If, as in figure 7*b*, *c* and *d* (but not figure 7*a*), there is no direct route from $\mathscr{B}$ states to $\mathscr{C}$ states then the results for $\boldsymbol{Q}_{\mathscr{B}\mathscr{C}} = \boldsymbol{0}$ given in (A 2.20)–(A 2.23) are still valid. It should be noted, however, that the lifetime of shut-blocked states, and the probability of re-opening after a blockage (from $\boldsymbol{G}_{\mathscr{C}\mathscr{A}}$; see A 2.22 and A 2.23), may depend on agonist (but not

blocker) concentration. For example if, as in figure 7*c*, there are three shut-blocked states, the time spent in RB and ARB will be long at low agonist concentration so a reduced slope of the 'blockage frequency' plot is expected even if equilibration among shut-blocked states is quite fast. At high agonist concentrations, however, most of the shut-blocked molecules would be in the fully liganded form (A_2RB) so the probability of re-opening will be increased and, unless A_2RB itself has a long lifetime, the slope of the plot of f against blocker concentration will be little reduced despite the existence of a route for shutting without re-opening. Similarly the open time per cluster and the number of bursts per cluster may be little reduced. When agonist and blocker are different molecules the 'blockage frequency' plot will be linear when the agonist concentration is held constant, but will have a slope that is reduced below k^*_{+B} to a greater extent, the lower the agonist concentration. When the agonist and the blocker are the same molecule, as in the present work, it is therefore predicted that the 'blockage frequency' plot will be nonlinear, with a slope that is reduced below k^*_{+B} at low agonist–blocker concentrations but which may approach k^*_{+B} at high concentration.

Other cases

In none of the above cases is the expected behaviour very sensitive to the existence of a direct route from blocked state, or states, to resting state, or states. For example, numerical calculations show that the schemes in figure 7*c* and *d* behave rather similarly in many circumstances; they will show differences in the structure of long gaps, but, given the complexity of the gap distribution in the presence of block and desensitization, these are likely to be difficult to interpret.

In cases where there is a direct route from $\mathscr{B}$ to $\mathscr{C}$ (as in figure 7*a* when shut-blocked states are short-lived) the full generality of (A 2.12)–(A 2.14) is needed. Various predictions are possible, depending on the details of the mechanism and on the numerical values of the rate constants. In some cases there will be no component in the distribution of shut times that can be clearly identified with blockages. When there is such a component the 'blockage frequency' plot will not necessarily have a slope less than k^*_{+B} despite the existence of a route for shutting of the blocked channel without re-opening. It can even exceed k^*_{+B}; this can happen, for example, if the main route for return from block without re-opening is via $A_2RB \rightarrow A_2R$. It is much more probable that A_2R will re-open (rather than returning to the resting state) so the cluster will continue.

Conclusions

For a simple channel blocker: (i) the reciprocals of the mean length of a single opening (m_0) and of the open time per burst (m'_0) should both increase linearly with blocker concentration (x_B), with slope k^*_{+B}; (ii) the mean open time per cluster (m_t) should be independent of x_B; (iii) the mean number of bursts per cluster (n_b) should increase linearly with x_B; and (iv) the 'blockage frequency' plot should have a slope of k^*_{+B}. Of the methods (ii)–(iv), only the 'blockage frequency' plot can be used when activations are so frequent that individual clusters are not clearly defined. For more complex mechanisms of block (i) should still be true, but m_t may fall with x_B, n_b may increase less than linearly with x_B, and the blockage frequency

plot may have a slope less than k^*_{+B}. In particular this will happen if there are shut-blocked states with long lifetimes. For mechanisms such as those in figure 7 such effects are likely to be more obvious at low agonist concentrations. The predicted behaviour of these mechanisms is not very sensitive to the existence of pathways from the blocked state, or states, to the resting state.

References

Adams, D. J. & Colquhoun, D. 1983 Current relaxations with high agonist concentrations. Do acetylcholine and suberyldicholine block ion channels in frog muscle? *J. Physiol., Lond.* **341**, 22–23*P*.

Adams, P. R. 1976 Relaxation of suberyldicholine-induced end-plate currents following voltage steps. *J. Physiol., Lond.* **256**, 19*P*.

Adams, P. R. 1977 Voltage jump analysis of procaine action at the frog end-plate. *J. Physiol., Lond.* **268**, 291–318.

Adams, P. R. & Sakmann, B. 1978 Decamethonium both opens and blocks endplate channels. *Proc. natn. Acad. Sci. U.S.A.* **75**, 2994–2998.

Colquhoun, D., Dreyer, F. & Sheridan, R. E. 1979 The actions of tubocurarine at the frog neuromuscular junction. *J. Physiol., Lond.* **293**, 247–284.

Colquhoun, D. & Hawkes, A. G. 1977 Relaxation and fluctuations of membrane currents that flow through drug-operated ion channels. *Proc. R. Soc. Lond.* B **199**, 231–262.

Colquhoun, D. & Hawkes, A. G. 1981 On the stochastic properties of single ion channels. *Proc. R. Soc. Lond.* B **211**, 205–235.

Colquhoun, D. & Hawkes, A. G. 1982 On the stochastic properties of bursts of single ion channel openings and of clusters of bursts. *Phil. Trans. R. Soc. Lond.* B **300**, 1–59.

Colquhoun, D. & Hawkes, A. G. 1983 The principles of the stochastic interpretation of ion channel mechanisms in *Single channel recording* (ed. B. Sakmann & E. Neher), pp. 135–175. New York: Plenum Press.

Colquhoun, D. & Ogden, D. C. 1984 Evidence from single-channel recording of channel block by nicotinic agonists at the frog neuromuscular junction. *J. Physiol., Lond.* **353**, 90*P*.

Colquhoun, D. & Sakmann, B. 1981 Fluctuations in the microsecond time range of the current through single acetylcholine receptor ion channels. *Nature, Lond.* **294**, 464–466.

Colquhoun, D. & Sakmann, B. 1983 Bursts of openings in transmitter-activated ion channels in *Single channel recording* (ed. B. Sakmann & E. Neher), pp. 345–364. New York: Plenum Press.

Colquhoun, D. & Sakmann, B. 1985 Fast events in single channel currents activated by acetylcholine and its analogues at the frog muscle end-plate. *J. Physiol., Lond.* (In the press.)

Colquhoun, D. & Sheridan, R. E. 1981 The modes of action of gallamine. *Proc. R. Soc. Lond.* B **211**, 181–203.

Colquhoun, D. & Sigworth, F. J. 1983 Fitting and statistical analysis of single channel records in *Single channel recording* (ed. B. Sakmann & E. Neher), pp. 191–263. New York: Plenum Press.

Gardner, P., Ogden, D. C. & Colquhoun, D. 1984 Conductances of single ion channels opened by nicotinic agonists are indistinguishable. *Nature, Lond.* **309**, 160–162.

Gurney, A. M. & Rang, H. P. 1984 The channel-blocking action of methonium compounds on rat submandibular ganglion cells. *Br. J. Pharmacol.* **82**, 623–642.

Hamill, O. P., Marty, A., Neher, E., Sakmann, B. & Sigworth, F. J. 1981 Improved patch-clamp techniques for high-resolution current recording from cells and cell-free membrane patches. *Pflügers Arch. Eur. J. Physiol.* **391**, 85–100.

Katz, B. & Miledi, R. 1978 A re-examination of curare action at the motor end-plate. *Proc. R. Soc. Lond.* B **203**, 119–133.

Lingle, C. 1983*a* Blockade of cholinergic channels by chlorisondamine on a crustacean muscle. *J. Physiol., Lond.* **339**, 395–417.

Lingle, C. 1983*b* Different types of blockade of crustacean acetylcholine-induced currents *J. Physiol., Lond.* **339**, 419–437.

Magleby, K. L. & Stevens, C. F. 1972 A quantitative description of end-plate currents. *J. Physiol., Lond.* **223**, 173–197.

Neher, E. 1983 The charge carried by single-channel currents of rat cultured muscle cells in the presence of local anaesthetics. *J. Physiol., Lond.* **339**, 663–678.

Neher, E. & Steinbach, J. H. 1978 Local anaesthetics transiently block currents through single acetylcholine-receptor channels. *J. Physiol., Lond.* **277**, 153–176.

Ogden, D. C. & Colquhoun, D. 1983 The efficacy of agonists at the frog neuromuscular junction studied with single channel recording. *Pflügers Arch. Eur. J. Physiol.* **399**, 246–248.

Ogden, D. C., Siegelbaum, S. A. & Colquhoun, D. 1981 Block of acetylcholine-activated ion channels by an uncharged local anaesthetic. *Nature, Lond.* **289**, 596–598.

Ogden, D. C., Siegelbaum, S. A. & Colquhoun, D. 1985 The effects of an uncharged local anaesthetic on acetylcholine-activated ion channels at the frog end-plate. (In preparation.)

Ruff, R. L. 1977 A quantitative analysis of local anaesthetic alteration of miniature end-plate currents and end-plate current fluctuations. *J. Physiol., Lond.* **264**, 89–124.

Sakmann, B., Patlak, J. & Neher, E. 1980 Single acetylcholine-activated channels show burst-kinetics in presence of desensitizing concentrations of agonist. *Nature, Lond.* **286**, 71–73.

Sigworth, F. J. 1982 Fluctuations of current through open ACh receptor ion channels. *Biophys. J.* **37**, 309a.

Sine, S. M. & Steinbach, J. H. 1984 Agonists block currents through acetylcholine receptor channels. *Biophys. J.* **46**, 277–283.

Yellen, G. 1984 Ionic permeation and blockade in Ca-activated K channels of bovine chromaffin cells. *J. gen. Physiol.* **84**, 157–186.